



ELSEVIER

Journal of
Environmental Radioactivity 53 (2001) 365–380

JOURNAL OF
ENVIRONMENTAL
RADIOACTIVITY

www.elsevier.com/locate/jenvrad

Full-spectrum analysis of natural γ -ray spectra

P.H.G.M. Hendriks*, J. Limburg, R.J. de Meijer

*Nuclear Geophysics Division, Kernfysisch Versneller Instituut, Rijksuniversiteit Groningen, Zernikelaan 25,
9747 AA Groningen, Netherlands*

Received 30 May 1999; received in revised form 30 October 1999; accepted 30 June 2000

Abstract

In this paper, a new system to measure natural γ -radiation in situ will be presented. This system combines a high-efficiency BGO scintillation detector with full-spectrum data analysis (FSA). This technique uses the (nearly) full spectral shape and the so-called ‘standard spectra’ to calculate the activity concentrations of ^{40}K , ^{232}Th and ^{238}U present in a geological matrix (sediment, rock, etc.). We describe the FSA and the determination of the standard spectra. Standard spectra are constructed for various geometries and a comparison in intensity and shape will be made. The performance of such a system has been compared to a more traditional system, consisting of a NaI detector in combination with the ‘windows’ analysis. For count rates typically encountered in field experiments, the same accuracy is obtained 10–20 times faster using the new system. This allows for shorter integration times and hence shorter measurements or a better spatial resolution. The applicability of such a system will be illustrated via an example of an airborne experiment in which the new system produced results comparable to those of much larger traditional systems. This paper will conclude with a discussion of the current status of the system and an outlook for future research. © 2001 Elsevier Science Ltd. All rights reserved.

Keywords: Natural γ -log analysis; In situ measurements; Spectral logger calibrations

1. Introduction

Natural radioactivity is a ubiquitous phenomenon on this planet and almost all substances are more or less radioactive. Measuring natural radioactivity is a complex subject with a number of inherent difficulties, especially when measuring in the field.

*Corresponding author. Tel.: +31-50-363-3565.

E-mail address: hendriks@kvi.nl (P.H.G.M. Hendriks).

The relevant radionuclides for the present applications are those of ^{40}K and the γ -ray emitting decay products in the decay series of ^{232}Th and ^{238}U .

One of the factors adding to the complexity of measuring natural radioactivity is that the decay series of ^{232}Th and ^{238}U are characterized more or less by an initial part dominated by α -decay and a part dominated by γ -ray emission. Questions related to the fulfilment of secular equilibrium, i.e. the activity concentrations are the same for all members of the decay chain, are difficult to check quantitatively. These questions are relevant for the determination of the content of Th and U by the activity of γ -ray emitting progeny. For all practical field applications, only γ -radiation is of importance, because α and β radiation is not very penetrating and will generally not escape the matrix and reach a (shielded) detector. The ^{232}Th and ^{238}U concentrations, derived from γ -ray measurements, are in general presented under the assumption of secular equilibrium.

Gamma-ray spectroscopy around the middle of this century focussed largely on γ -rays emitted by radionuclides produced in neutron, proton and α -induced reactions, using nuclear reactors and particle accelerators. Scintillation counters like NaI crystals were developed to analyse the complex γ -ray spectra by full-spectrum analysis; a time-consuming and laborious job, often carried out by hand in the absence of computers. A major breakthrough in this field was the almost simultaneous availability of semi-conductor detectors such as Ge(Li) and of computers. The high energy resolution of germanium detectors allowed the identification of the photopeaks of individual γ -rays and thereby the identification of weaker members in the particle-induced decay scheme. This advantage compensated for the lower detection efficiency compared to NaI detectors.

To measure natural γ -rays in the field, on the sea floor (De Meijer, Táncoz, & Stapel, 1996), in boreholes (Tittle, 1989), or land surfaces by direct contact or via airborne surveys (Darnley, 1991), various methods have been used. The choice of detector type is a trade-off between costs on the one hand and information flux in quantity and quality on the other. Until about a decade ago, scintillation detectors like NaI were quite generally used. They provide a combination of properties that made them suitable for many applications: relatively low price, available in large crystals, moderate resolution and operable at ambient temperatures. However, at the beginning of the 1990s, our group was confronted with the challenge to build a towable high-efficiency detector system to map sea floors (De Meijer, 1998). The detector should be radionuclide sensitive and its efficiency should be high enough to obtain sufficient statistics in about 10 s. Sea floors often contain low-activity sands with characteristic activity concentrations of about 200 Bq/kg ^{40}K , 5 Bq/kg ^{238}U , and 5 Bq/kg ^{232}Th .¹ These boundary conditions led to a detector system that had to be an order of magnitude more sensitive than the available systems such as the EEL of the British Geological Survey (Jones, 1994). These systems are based on NaI detectors, and the activities are derived from the γ -ray spectra using only the photopeak information.

¹ Activity concentrations are straightforwardly related to mass fractions: 1% K_2O = 314 Bq/kg ^{40}K , 1 ppm U = 12.25 Bq/kg ^{238}U and 1 ppm Th = 4.07 Bq/kg ^{232}Th .

To reach the goal, a detector system (MEDUSA) was designed, built and tested. The detector system consists of both an improved hardware and software part. In the hardware part, a large (15 cm long, 5 cm diameter), high-efficiency $\text{Bi}_4\text{Ge}_3\text{O}_{12}$, (bismuth germanate or BGO) detector was used rather than NaI, see the next section. In the software part, the improvement in sensitivity was achieved by including the full energy spectrum in the analysis (FSA) instead of the standard method of using ‘windows’ for the individual radionuclides.

This paper will briefly describe the relevant parts of the interactions of photons and matter to understand the detector properties and the shape of the γ -ray spectra. The methodology of FSA together with the characteristics and derivation of standard spectra will be treated. Furthermore, the performance of the FSA will be compared to the traditional ‘windows’ analysis. In this paper an application of the system and the interpretation of its results in geophysical quantities will be presented. At the end of the paper, directions for further development will be discussed.

2. Basic properties and methodology

2.1. Interaction processes

The FSA method is based on the basic properties of the interactions of γ -rays with matter. This paper therefore starts with an introduction that is necessary to comprehend the structure of γ -ray spectra measured with a certain type of detector. For more details, we refer to standard textbooks on γ -ray detection such as Leo (1987), Debertin and Helmer (1988) or Knoll (1989). In the following, we consider a piece of matter, either a detector or a geological matrix, in which γ -ray emitting radionuclides are incorporated. For natural γ -rays, with energies < 3 MeV, two types of interaction are relevant:

- *Photoelectric effect*: The photon is completely absorbed by a bound electron transferring all energy to the electron. The cross-section, in density units ($\text{m}^2 \text{kg}^{-1}$) depends on the γ -ray energy as E_γ^{-3} , with the atomic number as Z^n , with $n \sim 4-5$, and the material density ρ (in kg/m^3).
- *Compton effect*: The photon is (in)elastically scattered by an electron. The electron and the scattered photon share the incoming momentum. The cross-section ($\text{m}^2 \text{kg}^{-1}$) depends on the electron density and hence on ρ .

The third main interaction process of γ -rays with matter, pair production, only becomes important for $E_\gamma > 3$ MeV and is therefore not of interest for the study of natural radioactivity.

2.2. Detector types

The occurrence of these interactions in the matrix means that the intensity of γ -ray photons emitted with energy E_γ will be reduced when reaching the detector due

to scattering and absorption, and some of the photons will reach the detector with a lower energy. Additionally, these interactions will also take place in a detector, such that the spectrum of a mono-energetic γ -ray source will consist of a sharp peak (containing the γ -rays that have undergone the photoelectric-effect), and a continuum part at energies lower than the photopeak. The latter is named the Compton continuum. The intensity ratio between the peak and the continuum of a γ -ray emitted by the matrix will, as outlined above, depend on the photo energy (E_γ), the densities and Z -values of the matrix and the detector material, and also on the distance travelled by the γ -ray in the geological matrix. The slope of the continuum depends on the Z of the matrix and the detector.

Based on the properties of these processes, for a given γ -ray spectrum the optimum photopeak efficiency will be obtained for a large detector volume with high density and high Z -values. Detectors can roughly be divided into three types:

- *Semi-conductor detectors*, like hyper-pure germanium detectors (HPGe), with a high energy resolution, a moderate Z -value ($Z_{Ge}=32$) and moderate density ($\rho_{Ge}=5.3 \text{ g/cm}^3$).
- *'Inorganic' scintillation detectors*, such as NaI, CsI and BGO, with moderate energy resolutions, moderate to high densities ($\rho_{NaI}=3.7 \text{ g/cm}^3$, $\rho_{CsI}=4.5 \text{ g/cm}^3$, $\rho_{BGO}=7.1 \text{ g/cm}^3$) and components with high Z -values.
- *'Organic' scintillation detectors (plastics)*, with a low density ($\rho \approx 1 \text{ g/cm}^3$) and low Z -value.

The detectors are listed in the order of decreasing 'features'. HPGe spectra show sharp peaks on a relatively low continuum, whereas plastic detectors show a continuum with hardly any features. Scintillation detectors are somewhere in between these two extremes with broad peaks on a relative high continuum. It should be pointed out that the actual peak-to-Compton ratios of scintillation detectors are higher than for HPGe detectors, but due to the much better energy resolution of the HPGe detectors, the peaks protrude more prominently in the HPGe spectra.

For measuring natural γ -rays 'in situ', the need for liquid nitrogen (LN₂) cooling, the available crystal sizes and the moderate Z -values, limit the applicability of semi-conductor detectors. Therefore, they are predominantly used in the laboratory to measure the activity concentrations of natural radionuclides in samples. Plastic detectors have both a density and a Z -value that is too low to measure natural radioactivity in the field.

In this paper it will be shown that when combined with FSA, BGO ultimately is the logical choice of the inorganic scintillation detectors for measuring the, often low, concentrations of natural radionuclides in situ. BGO scintillator detectors are hardly used commercially for measuring natural γ -rays because they are more expensive than NaI, have a larger temperature gain-drift and a reduced energy resolution. However, the disadvantages of BGO relative to NaI were outweighed by the higher density and higher Z -value ($Z_I=53$ versus $Z_{Bi}=83$). Since the photo-effect scales with $Z^4 \left(\left(\frac{83}{53} \right)^4 \approx 6 \right)$, BGO detectors have a higher detection efficiency

and a better peak-to-Compton ratio, thereby reducing the acquisition time. Moreover, BGO is less brittle and, unlike NaI, not hygroscopic. To operate the MEDUSA BGO-detector, on-line software gain-drift stabilisation was developed.

3. Spectrum analysis methods

For the analysis of the spectra, in practice two methods are used: peak or window analysis and full-spectrum analysis (FSA). In the first method, the activity concentration is determined from the net content of the window around individual peaks. In the second method the shape of the total spectrum is taken into account and is ‘unfolded’ into the spectra for the individual radionuclides (the so-called standard spectra) and a background spectrum. It is more or less standard to analyse the HPGe spectra by the windows or peak method, and the plastic spectra by FSA. The best method to analyse spectra from inorganic scintillation detectors was investigated. The two methods differ in the sense that in the windows method only a region of interest of the spectrum is considered, namely the area around the most prominent peaks of the three nuclides, whereas the FSA method encompasses (almost) the full energy spectrum. Moreover, in the windows method, only the number of counts per window are considered, whilst in the FSA the structural features are included.

3.1. Windows analysis

The windows method is described for instance in a paper by Desbarats and Killeen (1990). Basically, the ^{40}K , ^{238}U and ^{232}Th concentrations, C_K , C_U and C_{Th} are expressed as

$$C_K = (n_K - \beta n_{Th} - \gamma(n_U - \alpha n_{Th}))/s_K, \quad (1)$$

$$C_U = (n_U - \alpha n_{Th})/s_U, \quad (2)$$

$$C_{Th} = n_{Th}/s_{Th}. \quad (3)$$

In these equations the quantities n_K , n_U and n_{Th} represent the counts in the windows for K, U and Th, respectively. These contents are detector and cosmic background (BG) corrected. Especially for low activities, the background subtraction becomes important and introduces a large uncertainty. Similarly, the relative uncertainties increase due to the propagation of uncertainties in the subtraction. The factors α , β and γ are the so-called stripping factors, and correct for Compton contributions of photopeaks at higher energies to lower windows. Forward stripping, i.e., spectral contributions to higher windows, is generally not taken into account but is important for high uranium–thorium ratios, see Desbarats (1990). The detection sensitivities in the respective windows are denoted by s_i and are extracted from calibrations.

3.2. Full-spectrum analysis

Another way to reduce the problem is the method of full-spectrum analysis (FSA). In this technique the (almost) full energy-spectrum is considered and the measured spectrum Y is described as the sum of the standard spectra X_j multiplied by the activity concentrations C_j for the individual radionuclides, plus a background spectrum (BG). Previous work along these lines has been carried out by, amongst others, Crossley (1982), Smith (1983) and Minty (1999, and references therein). However, as far as the authors are aware, this method has not been applied to BGO detectors.

The standard spectra are derived from separate calibration measurements and are in principle infinitely well-determined. The activity concentrations are quantities that follow from a fit of the calculated spectrum to the measured one. In the present approach, a least-squares procedure is used to find the optimal activity concentrations:

$$\chi^2 = \frac{1}{N - M} \sum_{i=1}^N [Y(i) - \sum_j C_j X_j(i) - BG(i)]^2 / w(i), \quad (4)$$

In Eq. (4), i is the channel (up to N), and $w(i)$ is a weight factor. The standard procedure takes the weight $w(i)$ as $Y(i)$. The number of standard spectra is given by M .

Comparing the windows and the FSA method, one notices that, by taking the full-energy spectrum, the sensitivity of the derived concentration to spectrum drift can be reduced. In the windows method an exactly determined set of equations is used for the calculation of the activity concentrations. Therefore, not enough parameters are available to monitor e.g. the quality of the gain-drift correction or the presence of additional radionuclides such as ^{137}Cs , whereas in the FSA a high χ^2 is indicative of (amongst others) incomplete gain-drift correction or an improper set of fitting functions. Additionally, for nuclides emitting more than one γ -ray, the part of the γ -rays that are not included into the windows will contribute to the quality of the result in the FSA as well.

4. Characteristics of standard spectra

4.1. Calibrations

The calibrations of the system are carried out under well-controlled laboratory conditions that mimic as closely as possible the experimental conditions, such as the solid angle coverage of the detector and density of the material matrix. The procedure is the same for both the windows analysis and the FSA. As an example, the calibrations for a borehole geometry will be treated, but the procedure itself is independent of geometry.

Table 1

Activity concentrations (in Bq/kg) of the four calibration drums used to determine the standard spectra for a borehole geometry

	^{40}K (Bq/kg)	^{232}Th (Bq/kg)	^{238}U (Bq/kg)
Silversand + KCl	1120 ± 20	0.87 ± 0.20	1.33 ± 0.19
Silversand + monazite	<2	351 ± 9	82 ± 2
Silversand + slags	25 ± 2	22 ± 1	395 ± 10
Silversand	0.89 ± 0.19	0.86 ± 0.03	1.54 ± 0.06

Three drums have been built at the KVI that contain a mixture of silversand (almost pure quartz) and a natural radioactive component: KCl for ^{40}K , phosphate slags for ^{238}U and monazite for ^{232}Th .

To assess the background radiation, a fourth drum has been filled with silversand only. The drum fillings were chosen to optimize the “orthogonality” of the calibration drums; thus each drum contains a high concentration of one natural radionuclide, and low concentrations of the other nuclides. The activities of the drums (in Bq/kg) were determined by measuring the activity concentrations of representative samples on a HPGe detector. The results are listed in Table 1.

This way, for each set-up, a 4×1 concentration matrix is constructed, containing the ^{40}K , ^{232}Th and ^{238}U concentrations and the background term that is always subtracted from each measured spectrum. Combined, this gives the total activity-concentration matrix A .

For calibration, the detector system is placed in each of the drums to measure the so-called calibration spectra (CS). These calibration spectra are the response of the detector to the known activity concentrations. Once the response of the detector to a known activity concentration is measured, the response to 1 Bq/kg of a radionuclide, i.e. the standard spectra (X), can be calculated according to

$$[CS] = [A][X]. \quad (5)$$

In principle, this procedure can be extended to include any nuclide of interest (such as ^{137}Cs). Moreover, as pointed out in an International Patent (1995), uncertainties in the measurements can also be propagated. The resulting standard spectra are shown in Fig. 1.

4.2. Background assessment

In general, the background radiation consists of several components: radionuclides that are present in the detector itself, sometimes radon in the surrounding air, and a cosmic part that depends on the geographic position and experimental conditions, e.g. in towed seabed experiments on the water depth. By depth monitoring during a survey it is possible to correct for this contribution.

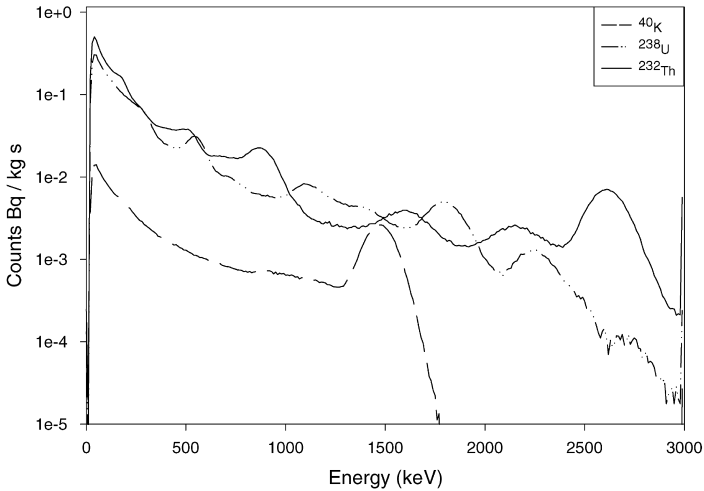


Fig. 1. Standard Spectra for ^{40}K (dashed), ^{238}U (dash-dot) and ^{232}Th (solid line) of the KVI/NGD MEDUSA detector (BGO) in a borehole geometry. The standard spectra are the response of the detector to 1 Bq/kg of a given radionuclide. To cover the wide range of count rates, the intensity (vertical axis) is plotted on a logarithmic scale; the γ -ray energy is plotted along the horizontal axis. This logarithmic scale reduces the structural differences.

The last background component is radiation introduced by the detector itself and ancillary equipment or supports. When measuring standard spectra indoors, construction materials (walls, floor) will also contribute; in outdoor experiments the detector can pick up γ -radiation originating from rock structures, surrounding walls, etc. This site-specific component can be corrected by the following procedure. First, the standard spectra are calculated according to Eq. (5), using the known radionuclide content in the calibration set-up. The resulting background standard spectrum may still contain contributions from the site-specific background. These standard spectra are used to assess the spurious ^{40}K , ^{232}Th and ^{238}U concentrations present in the background calibration spectrum. These concentrations are represented by δ . The concentration matrix A is adjusted accordingly to $A' = A + \delta$ and the standard spectra are calculated again via Eq. (5). This procedure is repeated until convergence is reached. Since the laboratory conditions used to reproduce real (infinite) conditions always have limited dimensions, and thus produce a different Compton background at low energy, the low-energy part of the standard spectra is excluded in the optimization procedure.

4.3. Geometry comparison

Thus far, the MEDUSA system has been calibrated in three geometries: borehole experiments, towed seabed and airborne surveys. For seabed and airborne geometry, calibrations were carried out at the pads of the BGS in Keyworth, United Kingdom.

For the borehole geometry the KVI drums were used. The various sets of standard spectra were used to investigate whether a simple scaling can be applied to convert borehole spectra to airborne or seabed spectra, or if the scaling factor is a function of γ -ray energy.

In Table 2, the total contents of the standard spectra (i.e. counts integrated from 100 keV to 3 MeV) for borehole, airborne and towed seabed geometries are given for all three natural radionuclides. The threshold of 100 keV was chosen to avoid electronics effects and differences in the lowest energy part of the Compton background. The ratios of the total contents, compared to the borehole standard spectra, for the different geometries are given in brackets.

From Table 2 it follows that the borehole standard spectra have the highest intensity, as was expected from the larger solid angle. The content ratios in Table 2 show that the scaling factor from borehole spectra to other geometries for ^{232}Th and ^{238}U has similar values, however for ^{40}K the scaling factor is roughly 20% higher. In the comparison of survey sample analysis on a HPGe and the MEDUSA system the 20% deficit is not found. The deviation is likely due to the chemically active KCl that was used for the drums causing inhomogeneities, and construction of a new calibration drum filled with potassium-rich feldspar is considered. From Table 2, one also notices that the standard spectra for an airborne system are more intense than for the seabed geometry. The only difference between these last two calibrations is that, in the seabed case, the detector is submerged and the increased attenuation and scattering of γ -rays in water (compared to air) will lead to a lower intensity and peak-to-Compton ratio.

The scaling factor discussed above is a scaling factor over the entire energy range, but the attenuation, and therefore the peak-to-Compton ratio, may differ for various geometries. The variations of the scaling factor over the energy range were therefore examined as well by calculating the ratios of the contents for each channel. This method, however, is susceptible to misalignments in the offset and alinearities in the energy mapping between the various standard spectra, as shown on the left-hand side of Fig. 2, where spurious peaks and valleys show up due to these effects.

Therefore, an alternative representation was chosen: the cumulative content of the standard spectra (i.e. the contents integrated upwards from a running threshold energy, and including the highest photopeak) was calculated for the three geometries and for the various natural radionuclides. In this way, the small-scale fluctuations

Table 2

Total contents of the standard spectra (i.e. counts integrated from 100 keV to 3 MeV) for borehole, towed seabed and airborne geometry, respectively^a

Configuration	^{40}K	^{232}Th	^{238}U
Borehole	0.25 (1)	5.18 (1)	3.86 (1)
Airborne	0.13 (0.52)	2.09 (0.40)	1.62 (0.42)
Towed seabed	0.11 (0.44)	1.90 (0.37)	1.40 (0.36)

^aIn brackets the ratios of the total contents with respect to the borehole geometry are given. The statistical uncertainty is less than a few percent.

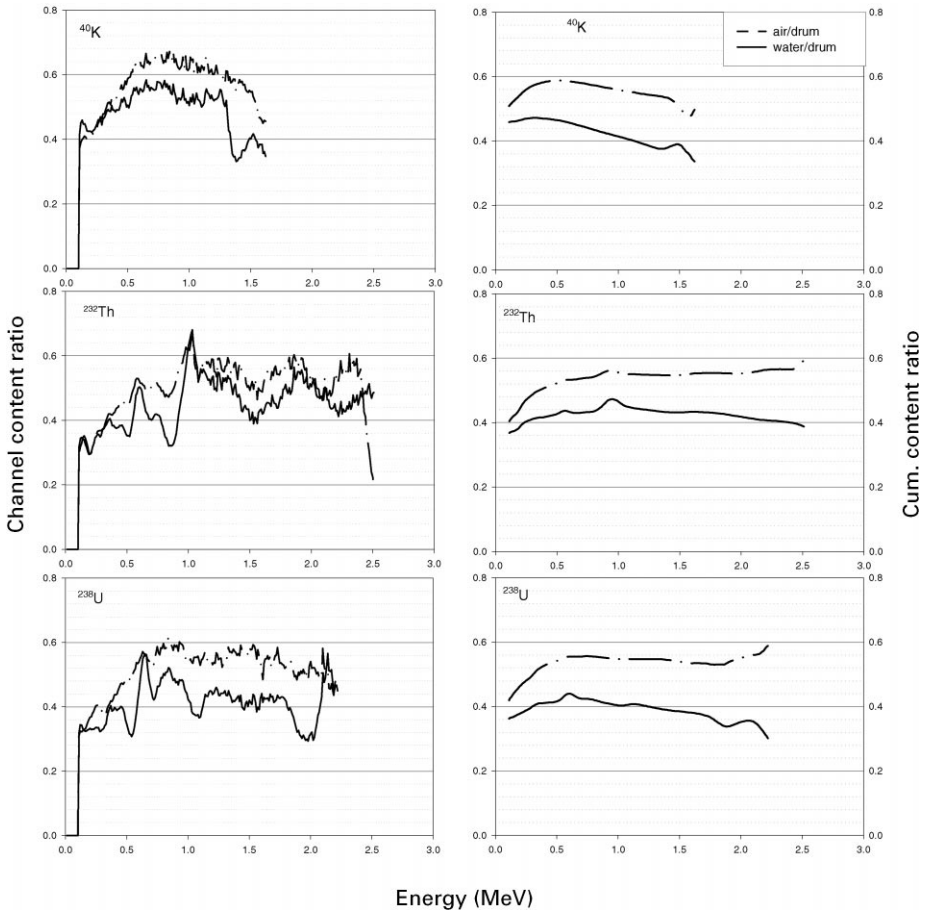


Fig. 2. Left three plots: ratios of channel contents for standard spectra for airborne (dash-dot) and seabed (solid line) geometries, for the natural radioisotopes potassium (top), uranium (middle) and thorium (bottom). The right-hand side shows the cumulative channel content ratios for different geometries of the standard spectra contents, integrated from the threshold energy to just above the photopeak energies. The ratios are shown with respect to the borehole geometry.

are smoothed out, while the variations in Compton continuum and photopeak area are preserved. The integration was carried out from threshold to last photopeak, rather than vice versa since the intensity of the spectra drops off sharply with energy, as can be seen in Fig. 1 where the standard spectra were given for the borehole geometry. This sharp drop-off also implies that, in the Compton part, the continuum is emphasized, and when reaching the photopeaks, the emphasis is on the photopeak content. The cumulative contents are shown as ratios with respect to the borehole geometry, on the right-hand side of Fig. 2. The value of the first data point corresponds to the values listed in Table 2.

Potassium has the simplest energy spectrum, a single photopeak located at 1461 keV and its Compton continuum. The right-hand side of Fig. 2 shows that for the Compton part of the potassium spectrum (up to 1400 keV) the ratios for both the airborne/borehole and the seabed/borehole geometry decrease with increasing energy, indicating that the Compton part is flatter for the borehole geometry. The variations around the average are about 10%. Therefore, scaling potassium standard spectra to other geometries can be done using a running scaling-factor if very high precision is required. The relative increase in intensity in the upper part of the Compton continuum of the borehole spectrum is caused by the increased Compton scattering in sand due to the higher Z -value and density of sand compared to water and air. For the ^{232}Th and ^{238}U spectra a running scaling-factor can be used as well, although the effect is less pronounced. This is because the energy spectra of these series contain multiple photopeaks, occasionally on a Compton continuum, which smears out the peak-to-Compton signal. If the accuracy needed is not better than $\pm 10\%$, an average scaling factor independent of γ -ray energy can be used for all three natural radionuclides. This means that only one calibration geometry is needed and that, via factors that, account for the differences between geometries, a calibration in one geometry can be adjusted for another.

4.4. Sensitivity analysis

In the previous sections, the traditional windows method and the full-spectrum analysis have been elucidated, together with the calibration procedure. To compare the performance of both analysis methods, data that were acquired from measuring in the monazite-filled calibration drum, have been analysed using both techniques. For more than 20,000 1 s spectra, the activity concentrations of ^{40}K , ^{232}Th and ^{238}U were calculated and plotted in histograms. In Fig. 3, an example of the distribution of calculated activities for ^{232}Th is given for an integration time of 4 s, for both the FSA as well as the windows method.

From these distribution plots, the mean values and widths were extracted. Additionally, spectra have been summed for various integration times, to create spectra with varying intensities and the aforementioned procedure was repeated. The results of this are shown in Fig. 3 as well, where the mean values of the histograms and the uncertainties are given for ^{40}K , ^{232}Th and ^{238}U as a function of counting statistics.

The concentrations given in the last three plots of Fig. 3 are the mean values from the distribution of a large number of calculated abundances. In general, as expected, these mean values correspond very well with the actual concentrations in the test sample as measured with a HPGe detector for both analysis techniques. However, for a given number of counts in the measured spectrum, the distribution spread (or uncertainty) is larger using the windows analysis, as can be seen in Fig. 3. These uncertainties represent the effects of the statistical scatter in the distribution of events over a spectrum (counting statistics).

In Fig. 4, the relative uncertainty in the thorium concentration is plotted as a function of counting statistics, for data analysed using FSA and for the windows method.

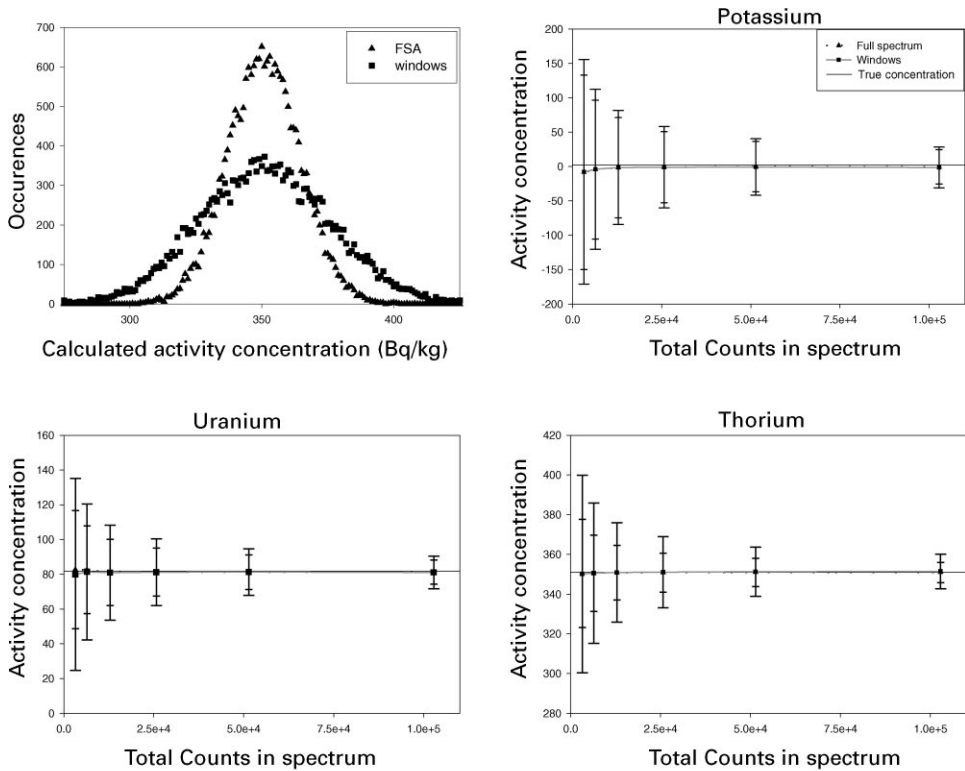


Fig. 3. An example of the distributions of the calculated activity concentrations as calculated with both the windows as well as full-spectrum analysis for a large number of a spectra (upper left corner). The mean value and spread of the distribution have been calculated for spectra as a function of the total number of counts and the results are shown as a function of statistics in the remaining three plots for ^{40}K , ^{232}Th and ^{238}U . In all plots, FSA data are indicated with triangles and windows data are squares.

Fig. 4 shows that, to obtain a similar accuracy as with the FSA, measuring times using the windows method need at least to be tripled. Moreover, this number increases as the intensity of the spectra decreases. When count rates become smaller, the propagation of uncertainties via the stripping factors defined in Eqs. (1)–(3) increases, especially since the highest energy window (thorium) for low count rates will induce a large uncertainty.

5. Application

Despite its initial purpose as a sea-floor radioactivity mapping system, the MEDUSA system was designed such that it could also be used in

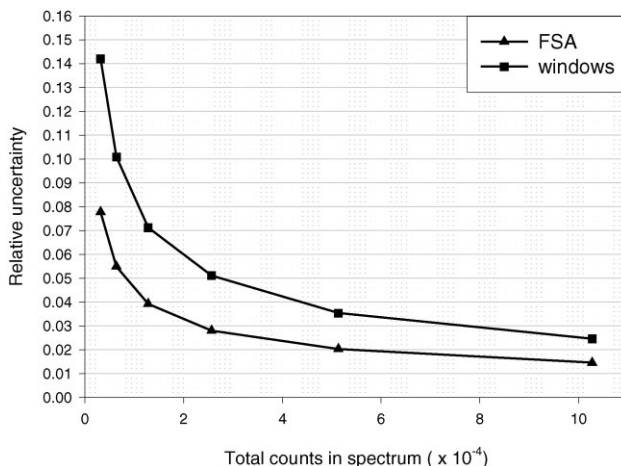


Fig. 4. The relative uncertainty in the activity concentrations of ²³²Th for spectra analysed according to the full-spectrum analysis (triangles) and traditional windows analysis (squares) as a function of counts in spectrum.

different settings, such as borehole logging and car or airborne surveys. In this section, a pilot-study that was carried out in co-operation with the South African Council for Geoscience (CGS) to apply the MEDUSA system in airborne surveys, will be described.

Airborne γ -ray spectroscopy allows the mapping of large areas in a short period. However, the method is expensive and the spatial resolution is rather poor, due to the high ground speed and altitude of the carrier. Using a microlight airplane as a survey platform, the costs per kilometer can be reduced by more than 50%, but the small payload (≈ 70 kg) of such a plane imposes severe demands on the detector system. Traditional systems, typically weighing about 235 kg, often consist of a package of four 4l NaI detectors that operate as individual detectors. In this way, the total detection volume and total detection efficiency are improved. However, the photopeak efficiency as well as the peak-to-Compton ratio remain the same as for a single 16l detector and are limited by the current maximum size of the crystals. Moreover, the background of the four detectors adds incoherently. On the other hand, the relatively small weight and size of MEDUSA (the detector system weighs a mere 2.8 kg), in combination with the short acquisition times, makes the system ideally suited to be used on the microlight platform.

An area of 5×15 km² in the vicinity of Carletonville (RSA) was covered with a line spacing of about 200 m. The area contains two tailing dumps of gold mines, with enhanced activity levels. In the Witwatersrand, gold and uranium occur as associated elements. In Fig. 5, the calculated thorium (color scale 0–540 Bq/kg) and uranium (range 0–840 Bq/kg) concentrations are shown.

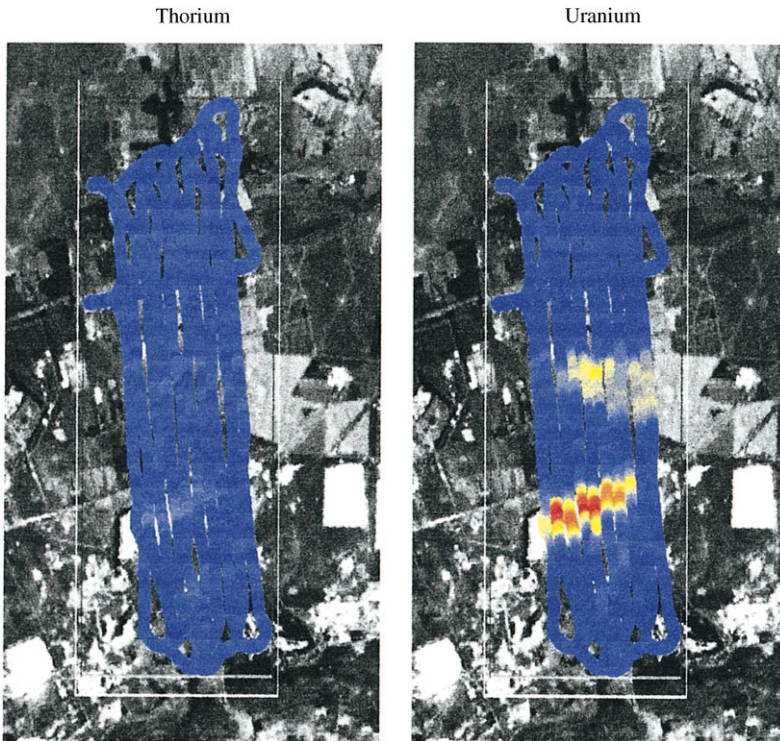


Fig. 5. The uranium and thorium concentrations as measured with the 2.8 kg airborne MEDUSA system near Carletonville, RSA. The data are overlaid on satellite pictures of the surveyed area.

An overlay with satellite pictures of the area clearly identifies the measured hot spots as the former gold-mine dumpsites. Furthermore, since the system is nuclide-specific, the enhanced radioactivity levels can be attributed to uranium, a residue of gold production. Although the thorium and uranium standard spectra resemble one another in the continuum part, still both nuclides can be separated well with the current system, as can be seen in Fig. 5.

These data were collected as part of a feasibility study and the aim was to acquire a data set that could be compared to data acquired using a commercial airborne system. Unfortunately, due to circumstances, a follow-up survey in which concurrent measurements with MEDUSA and a traditional system are done could not be carried out up to now. Still, the data show that the dynamic range of the MEDUSA system delivers a data quality similar to that of a much heavier commercial system, but at a more cost-effective rate. Finally, the MEDUSA measurements were carried out with a system consisting of a single BGO crystal that is neither optimized in size or geometry for this purpose. Therefore, the data quality of this system can still be improved via optimizing the detector shape and dimensions.

6. Conclusions and outlook

The high detection efficiency of a BGO detector, together with a full-spectrum analysis of the γ -ray spectra makes the MEDUSA system at least one order of magnitude more sensitive than traditional systems based on NaI detectors and ‘windows’ analysis. This is on the one hand due to the four to five times higher efficiency of BGO compared to NaI. On the other hand, the advanced data analysis increases the sensitivity by an extra factor of at least three. When count rates become smaller, the difference in sensitivity between the new system and traditional systems grows progressively, due to the propagation of errors via the stripping factor in the windows method, notably so for the higher energies (uranium and thorium).

The improved sensitivity allows for smaller integration times, hence shorter measurements or a higher spatial-resolution. This makes MEDUSA very suited to measure the generally low-activity concentrations of naturally occurring radionuclides in situ, such as towed seabed, borehole logging or airborne surveys. This was illustrated by an example of an airborne survey, where the MEDUSA system consisting of a single 2.8 kg BGO crystal delivers data quality similar to that of a package of, in total 235 kg, heavy traditional systems. Optimization of the shape and dimensions of the BGO detector for this purpose will improve the data quality of the MEDUSA system further.

A disadvantage of FSA is that the uncertainties in the derived activity concentrations are influenced by the covariances between the standard spectra for ^{40}K , ^{232}Th and ^{238}U , which are increased compared to the windows method. The increased covariances are caused by the inclusion of the Compton part of the γ -ray spectrum. The covariance is most important for U and Th since their spectra are most similar in the continuum part. Further research to reduce the covariance is in progress.

If the desired accuracy is in the range of 10%, the standard spectra determined for one geometry can be adjusted to the appropriate geometry, independent of γ -ray energy. If a better accuracy is needed, a scaling factor that varies with energy should be used for conversion of standard spectra. This is important because only *one* calibration environment is now necessary, and a scaling factor encompassing the geometry effects can be used to convert the standard spectra for the other geometries. Recently, Monte Carlo simulations of γ -ray transport have started. The goal of the new investigation is to better understand the shape of the γ -ray spectra as recorded by the detector. We anticipate being able to extract from the measured spectra information on density variations and/or layer structures in the geological matrix. In the longer term, we intend to check these achievements by ground truthing. Eventually, we aim at combining the γ -ray information with other physical parameters to improve the geological information.

Acknowledgements

The authors would like to express their appreciation and thank Ron ten Have, Cees Stapel and Lars Venema for their contributions to the work presented in this paper.

References

- Crossley, D. J., & Reid, A. B. (1982). Inversion of gamma ray data for element abundances. *Geophysics*, 47, 117–126.
- Darnley, A. G. (1991). The development of airborne gamma ray spectrometry: case study in technological innovation and acceptance. *Nuclear Geophysics*, 5(4), 377–402.
- Desbarats, A. J., & Killeen, P. G. (1990). A least-squares inversion approach to stripping in gamma-ray spectral logging. *Nuclear Geophysics*, 4(3), 343–352.
- Debertin, K., & Helmer, R. G. (1988). *Gamma- and X-ray spectrometry with semiconductor detectors*. Amsterdam: Elsevier Science Publishers B.V.
- Jones, D.G. (1994). *Towed seabed gamma ray spectrometre: EEL is a radiometric instrument for wide range of offshore mineral exploration, environmental survey applications*. Sea Technology, August (pp. 89–93).
- Minty, B. R. S., Mc Fadden, P., & Kennet, B. L. N. (1999). Multichannel processing for airborne gamma-ray spectrometry. *Geophysics*, 63(6), 1971–1985.
- De Meijer, R.J., Tánčzos, I.C., & Stapel, C. (1996). *Radiometry as a technique for use in coastal research*. Geology of Siliciclastic Shelf Seas, Geological Society Special Publication No 117 (pp. 289–297).
- De Meijer, R. J. (1998). Heavy minerals: From ‘Edelstein’ to Einstein. *Journal of Geochemical Exploration*, 62, 81–103.
- International Patent Application WO 95/27223, 1995 .
- Knoll, G.F. (1989). *Radiation detection and measurement*. New York: Wiley.
- Leo, W. R. (1987). *Techniques for nuclear and particle physics experiments*. Berlin: Springer.
- Smith, H.D., Robbins, C.A., Arnold, D.V., Gadokan, L.L., & Cealon, J.G. (1983). *A multi-function compensated spectral natural gamma ray logging system*. Society of Petroleum Engineers SPE 12050.
- Tittle, C. W. (1989). A history of nuclear well logging in the oil industry. *Nuclear Geophysics*, 3(2), 75–85.